

Supporting Information

¹ Pulsed laser deposition of Bi₂S₃/CuInS₂/TiO₂ cascade structure for high photoelectrochemical performance

Minmin Han^{a,b}, Junhong Jia^{a,*}, Wenzhen Wang^{a,*}

^a State Key Laboratory of Solid Lubrication, Lanzhou Institute of Chemical Physics, Chinese Academy of Sciences, Lanzhou, 730000, P. R. China.

^b University of Chinese Academy of Sciences, Beijing, 100080, P. R. China.

* Corresponding author. Tel./Fax: +86-931-4968611.
E-mail address: jhjia@licp.cas.cn (J. Jia)

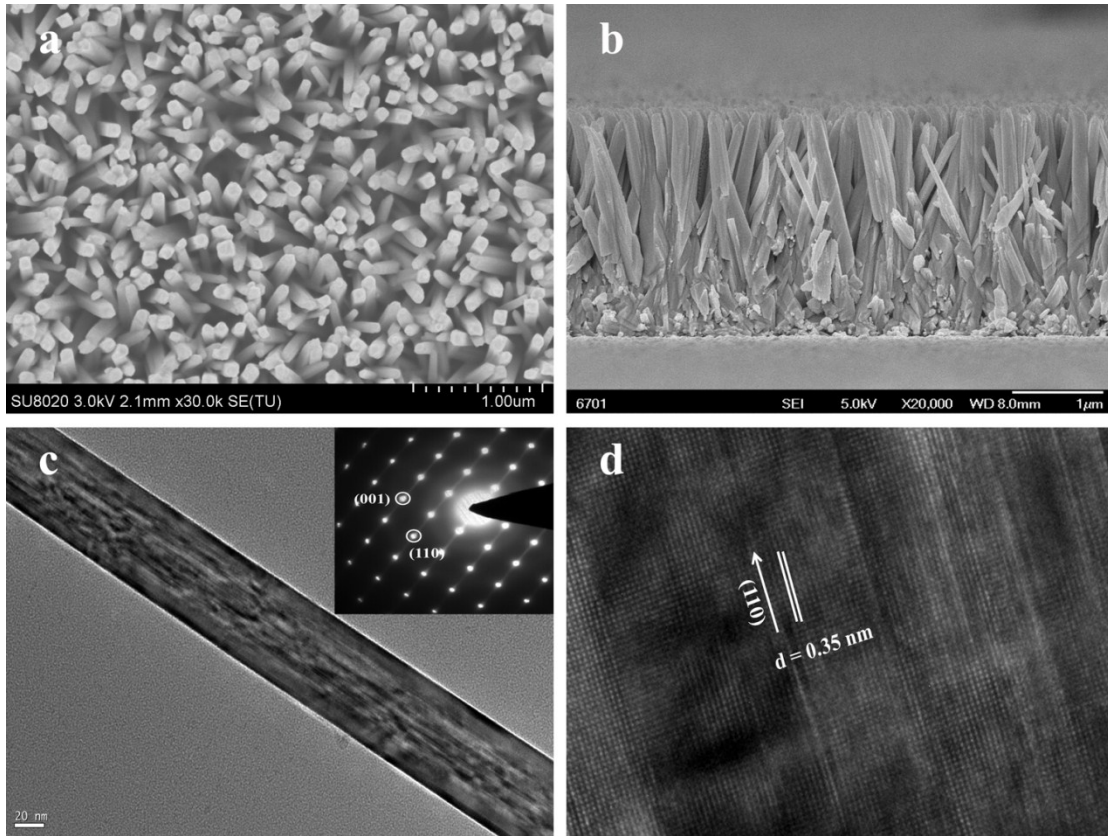


Fig. S1 Typical top-view (a) and cross-section view (b) FESEM images of plain TiO₂ nanorods. TEM (c) and HRTEM (d) images of TiO₂ nanorods, the inset in (c) is the selected-area electron diffraction pattern of TiO₂ nanorods.

Fig. S1a shows a typical top-view FESEM image of the plain TiO₂ nanorods. The TiO₂ nanorods with tetragonal crystal planes grow uniformly all over the FTO substrate with an obvious porosity between them. The cross-sectional view (Fig. S1b) demonstrates that the TiO₂ nanorods are vertically aligned and the length of TiO₂ nanorods is about 2 μm . Fig. S1c and d show the TEM and HRTEM images of the plain TiO₂ nanorods. It can be found that the diameter of plain TiO₂ nanorod is around 110 nm (Fig. S1c). The SAED pattern (the inset in Fig. S1c) and the HRTEM image (Fig. S1d) confirm that the nanorods are single crystalline. The HRTEM image shows a (110) lattice spacing of 0.35 nm, and the nanorods grow along the (110) crystal

plane with a preferred (001) orientation. The X-ray diffraction (XRD) spectrum displayed in Fig. 1f also confirms the single crystalline nature of TiO₂ nanorods, and the nanorods can be classified as tetragonal rutile phase (JCPDS file no. 21-1276) as all the characteristic peaks of TiO₂ nanorods agree well with rutile phase.

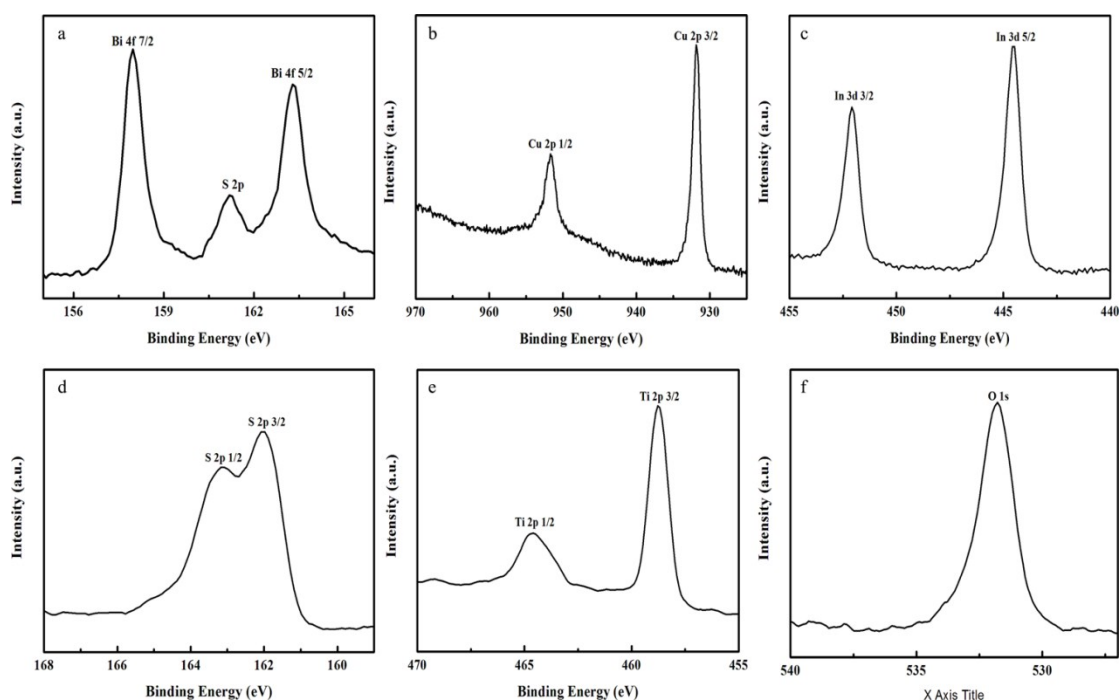


Fig. S2 High-resolution XPS spectra of BS(300)/CIS(350)/TiO₂: (a) Bi 4f, (b) Cu 2p, (c) In 3d, (d) S 2p, (e) Ti 2p and (f) O 1s.

In order to determine the composition and valence state of elements in BS(300)/CIS(350)/TiO₂, the XPS analysis is conducted as shown in Fig. S2. The elements binding energy of high resolution spectrum was revised refer to the binding energy of C1s (284.8 eV). Fig. S2a shows the high-resolution spectrum of Bi4f, the peaks of which is located in 158.5 eV (Bi 4f_{7/2}) and 163.8eV (Bi 4f_{5/2}), which are in agree with that of Bi₂S₃ in literature.¹ As shown in Fig. S2b, the binding energies of 931.9 eV (Cu 2p_{3/2}) and 951.8 eV (Cu 2p_{1/2}) are consistent with Cu (I). The binding energies of In 3d are 444.5 eV (In 3d_{5/2}) and 452.08 eV (In 3d_{3/2}), suggesting the

presence of In (III) (Fig. S2c). The close up survey in S 2p region (161.8 eV) doublet peaks locate at 161.38 eV (S 2p_{3/2}) and 162.5 eV (S 2p_{1/2}) with an energy difference of 1 eV (Fig. S2d), which are assigned to S coordinated to Cu and In.² Moreover, the peaks of the binding energies at 458.7 eV and 464.6 eV were assigned to Ti 2p_{3/2} and Ti 2p_{1/2} (Fig. S2e), which are attributed to that of crystalline rutile TiO₂, and the binding energy of the O 1s peak displayed in Fig. 3f at about 532.1 eV corresponds to that of O in TiO₂.³

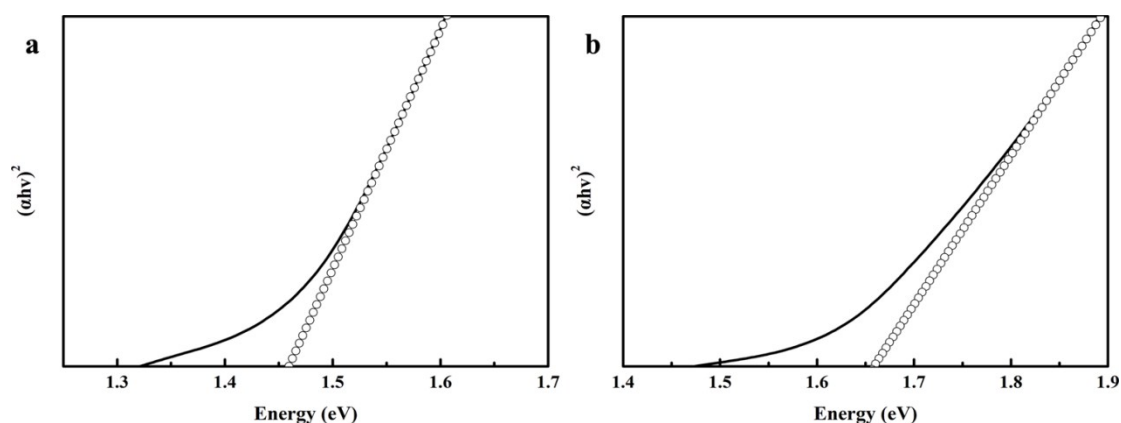


Fig. S3 The plots of $(\alpha h\nu)^2$ against photon energy ($h\nu$) for BS(300) films (a) and CIS(350) films (b).

Fig. S3 shows the plots of $(\alpha h\nu)^2$ against photon energy ($h\nu$) for BS(300) films and CIS(350) films, and the band gap of Bi₂S₃ QDs and CuInS₂ QDs is determined to be 1.46 eV and 1.66 eV respectively according to the long wavelength extrapolation of the band gap. Compared with that of the bulk Bi₂S₃ and CuInS₂, the band gaps of the two QDs all have changed, suggesting the presence of quantum size effect.

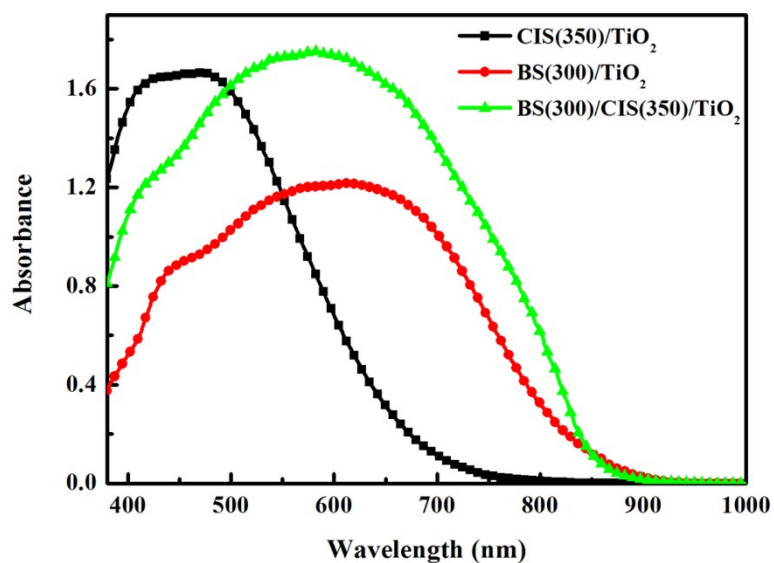


Fig. S4 UV-vis absorption spectra of various photoelectrodes.

Table S1 Photovoltaic parameters of QDSSCs assembled with BS(300)/CIS(350)/TiO₂ and BS(300)/TiO₂ photoelectrodes (each group has 5 devices in parallel).

Samples	V _{OC} (V)	J _{SC} (mA/cm ²)	FF	η (%)
BS(300)/CIS(350)/TiO ₂	0.49	19.62	0.50	4.81
	0.48	19.55	0.49	4.57
	0.47	19.63	0.50	4.60
	0.49	19.65	0.48	4.67
	0.47	20.29	0.49	4.70
	0.46	15.84	0.45	3.31
BS(300)/TiO ₂	0.46	15.61	0.46	3.28
	0.45	15.78	0.46	3.27
	0.47	15.79	0.45	3.29
	0.45	16.12	0.46	3.31

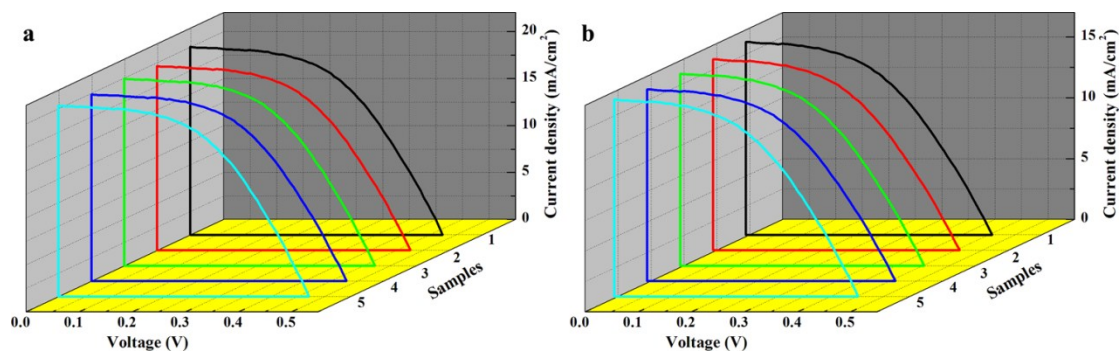


Fig. S5 J-V characteristics (b) of QDSSCs assembled with (a) BS(300)/CIS(350)/TiO₂ and (b) BS(300)/TiO₂ photoelectrodes (each group has 5 devices in parallel).

REFERENCES

- (1) Y. Huang, G. Xie, S. Chen and S. Gao, *Journal of Solid State Chemistry*, 2011, 184, 502-508.
- (2) Y. Shi, Z. Jin, C. Li, H. An, J. Qiu, *Appl. Surf. Sci.* 252 (2006) 3737.
- (3) D. Huang, Z. D. Xiao, J. H. Gu, N. P. Huang, C. W. Yuan, *Thin Solid Films* 305 (1997) 110.